

## Magneto-gyrotropic photogalvanic effects due to inter-subband absorption in quantum wells

H Diehl<sup>1</sup>, V A Shalygin<sup>2</sup>, S N Danilov<sup>1</sup>, S A Tarasenko<sup>3</sup>, V V Bel'kov<sup>3</sup>,  
D Schuh<sup>1</sup>, W Wegscheider<sup>1</sup>, W Prettl<sup>1</sup> and S D Ganichev<sup>1</sup>

<sup>1</sup> Terahertz Center, University of Regensburg, 93040 Regensburg, Germany

<sup>2</sup> St Petersburg State Polytechnic University, 195251 St Petersburg, Russia

<sup>3</sup> A F Ioffe Physico-Technical Institute, Russian Academy of Sciences,  
194021 St Petersburg, Russia

E-mail: [sergey.ganichev@physik.uni-regensburg.de](mailto:sergey.ganichev@physik.uni-regensburg.de)

Received 30 July 2007, in final form 21 September 2007

Published 9 October 2007

Online at [stacks.iop.org/JPhysCM/19/436232](http://stacks.iop.org/JPhysCM/19/436232)

### Abstract

We report on the observation of the magneto-photogalvanic effect (MPGE) due to inter-subband transitions in (001)-oriented GaAs quantum wells. This effect is related to the gyrotropic properties of the structures. It is shown that inter-subband absorption of linearly polarized radiation may lead to spin-related as well as spin-independent photocurrents if an external magnetic field is applied in the plane of the quantum well. The experimental results are analysed in terms of the phenomenological theory and microscopic models of MPGE based on either asymmetric optical excitation or asymmetric relaxation of carriers in  $k$ -space. We observed resonant photocurrents not only at oblique incidence of radiation but also at normal incidence, demonstrating that conventionally applied selection rules for the inter-subband optical transitions are not rigorous.

Optical excitation of free carriers can lead to generation of an electric current in a nominally unbiased semiconductor structure. In this paper we deal with the photogalvanic effects, which appear neither due to inhomogeneity of the optical excitation nor due to inhomogeneity of the sample (in the case of quantum well structure we mean in-plane inhomogeneity). Such photocurrents are caused by the asymmetry of elementary processes of photoexcitation or carrier relaxation resulting in a redistribution of carriers in momentum space. This is possible in structures of the appropriate symmetry only; in particular, gyrotropic materials give a rich spectrum of photogalvanic phenomena. In gyrotropic quantum well structures (QWs) photocurrents comprise (for a review, see [1–3]) the linear [4] and circular [5–8] photogalvanic effects, the linear and circular photon drag effects [9–11], the spin-galvanic effect due to optical excitation [12, 13], as well as photocurrents caused by quantum interference of one- and two-photon excitation [14–17], which represent coherent photogalvanic effects [18, 19]. These investigations explored new mechanisms of photocurrent formation and gave experimental

access to in-plane symmetry properties, spin relaxation, and details of band structure, and in particular to relativistic spin-orbit features of low-dimensional structures like Rashba and Dresselhaus spin-splitting in semiconductor quantum wells [20, 21].

An additional root of photogalvanic effects is provided by the application of an external magnetic field. The magnetic field breaks the time inversion symmetry, resulting in additional mechanisms of photocurrents. For instance, in inversion asymmetric but non-gyrotropic bulk crystals like GaAs, homogeneous illumination with circularly polarized radiation does not yield a current. However, in the presence of an external magnetic field this effect becomes possible and has been detected [22]. Essential progress has been achieved in the generation of magnetic field induced photogalvanic effects applying visible, near-, mid- and far-infrared laser radiation (for a review, see [2, 3, 23]). It has been demonstrated that optical excitation of quantum well structures can result in spin photocurrents, caused by the Drude absorption due to spin-dependent asymmetric scattering [24–26] or direct optical transitions between branches of the spin-split electron subband [27, 28], as well as in photocurrents due to spin-independent diamagnetic mechanisms [29–32].

Here we present experimental and theoretical studies of photocurrents induced by inter-subband optical transitions in quantum wells in the presence of an in-plane magnetic field. In contrast to the inter-band excitation, here we deal with monopolar currents because only one type of carrier, conduction electrons, is involved in the photoexcitation. The analysis gives evidence that the observed photocurrents are related to gyrotropy of quantum wells, which is caused by bulk and/or structure inversion asymmetry. The gyrotropic point-group symmetry makes no difference between components of axial and polar vectors, and hence allows an electric current  $j_\alpha \propto I B_\beta$ , where  $I$  is the light intensity inside the sample and  $B_\beta$  are components of the applied magnetic field. Photocurrents which simultaneously require gyrotropy and the presence of a magnetic field are gathered in a class of magneto-optical phenomena denoted as magneto-gyrotropic photogalvanic effects [2, 3]. We demonstrate that the magneto-gyrotropic photogalvanic effect generated by direct transitions between size-quantized subbands is caused by a new, so far undiscussed, type of spin-independent diamagnetic mechanism. We show that the current is due to  $k$ -linear diamagnetic terms in the scattering amplitude which describe the relaxation of photoexcited carriers.

## 1. Experimental results

Experiments have been carried out on molecular-beam-epitaxy grown (001)-oriented n-doped GaAs/AlGaAs multiple (30 periods) QWs at room temperature and liquid helium temperature. Each quantum well of 8.8, 8.2, and 7.6 nm width contains a two-dimensional electron gas with a carrier density of  $3 \times 10^{11} \text{ cm}^{-2}$  at 4.2 K. The quantum well widths are chosen to be around 8 nm so that the separation between the lowest ( $e1$ ) and the second ( $e2$ ) conduction subbands matches the photon energy range of a CO<sub>2</sub> laser [13, 33, 34]. In order to correlate the spectral dependence of the photocurrent to the absorption of the QWs, optical transmission measurements have been performed using a Fourier transform infrared spectrometer. Direct inter-subband optical transitions in  $n$ -type GaAs QWs are obtained by applying various wavelengths of a line tunable Q-switched laser as well as a transversal excited atmospheric pressure (TEA) CO<sub>2</sub> laser (see, e.g. [3, 35]). The lasers yield linearly polarized radiation at wavelengths  $\lambda$  of between 9.2 and 10.8  $\mu\text{m}$  corresponding to photon energies  $\hbar\omega$  ranging from 135 to 114 meV. The Q-switched laser has a peak power of 2 kW at a repetition rate of 300 Hz.

The samples are irradiated at normal incidence, i.e. along the growth direction, as well as at oblique incidence with an angle  $\theta_0$  between the light propagation direction and the QW growth direction  $z$ . Here we use Cartesian coordinates  $x \parallel [110]$ ,  $y \parallel [1\bar{1}0]$ ,  $z \parallel [001]$ . An

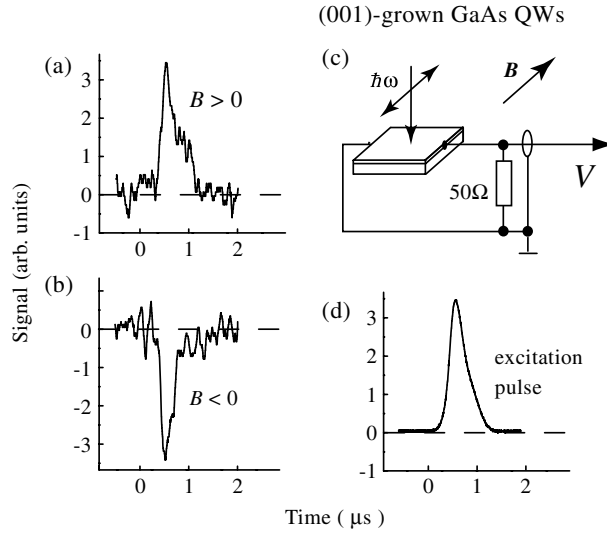


**Figure 1.** Oscilloscope traces obtained for pulsed excitation of (001)-grown *n*-type GaAs QWs at  $\lambda = 10.27 \mu\text{m}$ . Figures (a) and (b) show magneto-gyrotropic photogalvanic signals obtained for magnetic fields  $B_y = 0.3$  and  $-0.3$  T, respectively. For comparison, in (d) a signal pulse of a fast photon drag detector is plotted. In (c) the measurement arrangement is sketched.

external magnetic field  $\mathbf{B}$  up to 1 T is applied parallel to the interface plane along the  $x$  or  $y$  directions. In order to vary the angle between the polarization vector of the linearly polarized light and the magnetic field, we place a linear polarizer, made of two Brewster windows, behind a Fresnel rhomb. After passing through the Fresnel rhomb, initially linearly polarized laser light becomes circularly polarized. Rotation of the linear polarizer enables us to obtain linearly polarized radiation with an angle  $\alpha = 0^\circ\text{--}360^\circ$  between the vector of light polarization and the incidence plane.

To measure electric currents, two pairs of Ohmic contacts have been centred at opposite sample edges oriented along  $x$  and  $y$  (see figure 1(c)). The photocurrent  $J$  generated in the unbiased devices is measured via the voltage drop across a  $50 \Omega$  load resistor in a closed-circuit configuration (see figure 1(c)). The voltage in response to a laser pulse is recorded with a fast storage oscilloscope.

Irradiation of samples with normally incident linearly polarized radiation in the absence of an external magnetic field causes no photocurrent. This result agrees with the phenomenological theory, which does not allow any photocurrent at homogeneous excitation of structures belonging to  $D_{2d}$  or  $C_{2v}$  point-group symmetries relevant to (001)-grown GaAs QW structures [1–3]. A photocurrent response is obtained only when a magnetic field  $\mathbf{B}$  is applied. The signal is detected only in the direction perpendicular to the orientation of the magnetic field independently of whether  $\mathbf{B}$  is aligned along  $x$  or  $y$ . The basic features of the signals remain the same in both geometries, therefore in the following we give only results for photocurrents measured in the  $x$  direction and a magnetic field oriented along  $y$ . The signal follows the temporal structure of the laser pulse and changes the sign upon inversion of the magnetic field direction from  $B_y > 0$  to  $B_y < 0$ . Signal traces are shown in figure 1 compared to records of a linear photon drag detector [3]. Besides the experimental geometry with normal incidence of the radiation on the samples, the magnetic field induced photocurrent has also been observed at oblique incidence. We note that the excitation of QWs at oblique incidence results

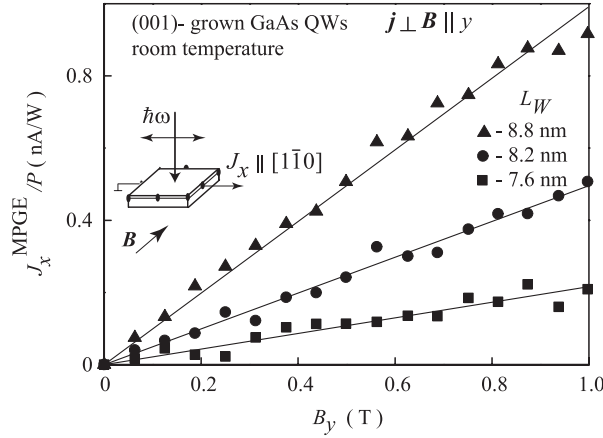


**Figure 2.** Magnetic field dependence of the photocurrent measured in (001)-grown GaAs QWs of various widths on the magnetic field  $B$  parallel to the  $[1\bar{1}0]$  axis. Optical excitation of  $P \approx 1$  kW at normal incidence is applied at three different wavelengths corresponding to the signal maximum in each QW; see arrows in figure 4 ( $\lambda_1$  for QW with  $L_W = 8.8$  nm,  $\lambda_2$  for  $L_W = 8.2$  nm and  $\lambda_3$  for  $L_W = 7.6$  nm). The current is measured in the direction perpendicular to  $B$  and for radiation polarized perpendicular to  $B$ .

in a measurable electric current even at zero magnetic field due to the linear photogalvanic and photon drag effects [3]. In this work we examine magnetic field induced photocurrents  $J_x^{\text{MPGE}}$  only, i.e. currents which reverse their sign upon switching the magnetic field direction. In order to extract such a current contribution from the measured total current we determine the response to the magnetic field aligned along the  $y$  axis,  $B_+$ , and along  $-y$ ,  $B_-$ , and evaluate the data after

$$J_x^{\text{MPGE}} = [J_x(B_+) - J_x(B_-)] / 2. \quad (1)$$

Magnetic field and polarization dependences of  $J_x^{\text{MPGE}}$  are presented in figures 2 and 3. As is shown in figure 2, the photocurrent exhibits a linear dependence on the magnetic field strength in all investigated samples. Figure 3 demonstrates the essential difference between the magnetic field induced photocurrents excited at normal incidence and at oblique incidence. While at normal incidence the current is almost independent of the radiation polarization, at oblique incidence the magneto-induced photocurrent becomes polarization-dependent: it reaches a maximum for the radiation polarized in the incidence plane (p-polarization,  $\alpha = 0^\circ$ ) and a minimum for the orthogonal polarization where the radiation electric field has no component normal to the QW plane (s-polarization,  $\alpha = 90^\circ$ ).

Figure 4 shows the spectral dependences of the photocurrent obtained in the range of photon energies accessible with the  $\text{CO}_2$  laser. The data are obtained at normal incidence for a constant magnetic field  $B = 0.3$  T in QW structures of various QW widths  $L_W$ . It is seen that the photocurrent has a resonant character and the peak of the resonance shifts to the higher energies for narrower QWs. In figure 5 the observed current for a sample with QWs with a width of 8.8 nm is plotted as a function of photon energy  $\hbar\omega$  together with the absorption spectrum. The spectral dependence of the photocurrent corresponds to that of inter-subband absorption measured by means of the Fourier transform infrared spectroscopy and can be well fitted by a Lorentzian. The photocurrent resonance shifts to shorter wavelength (blue shift) and narrows if the temperature is reduced from room temperature to liquid helium temperature. All the observed features, the coincidence of the photocurrent and the absorbance spectra, the

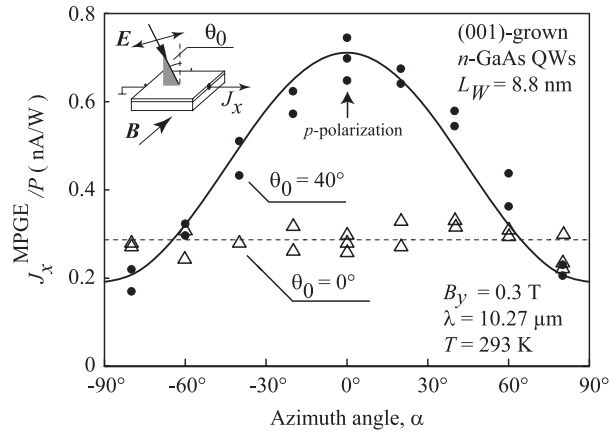


**Figure 3.** Dependences of the magneto-induced photocurrent  $J_x^{\text{MPGE}}$  normalized by the power  $P$  on the azimuth angle  $\alpha$  of the light polarization plane measured at normal incidence ( $\theta_0 = 0^\circ$ ) and at oblique incidence ( $\theta_0 = 40^\circ$ ). In the latter case the plane of incidence is the  $(xz)$  plane. Azimuth angle  $\alpha = 0^\circ$  corresponds to the maximum value of the electric field component normal to the QW plane (p-polarization). Solid and dashed curves are fits by an analytical expression given by equation (3) taking into account the light refraction and absorption in the QW structure (see equation (2)).

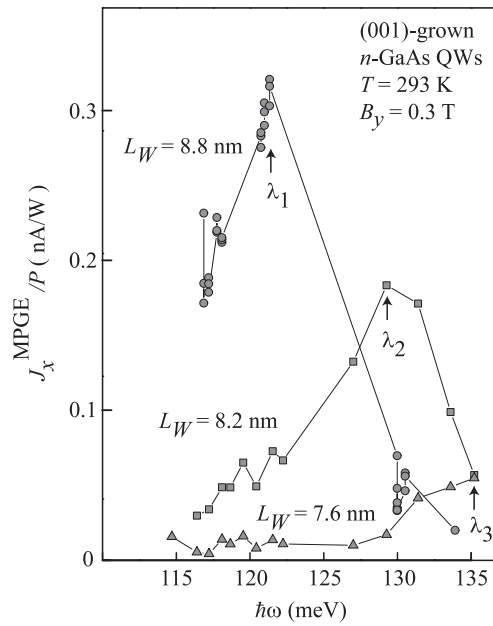


**Figure 4.** Spectral dependences of the magneto-induced photocurrent  $J_x^{\text{MPGE}}$  normalized by the power  $P$  at the magnetic field  $B_y = 0.3$  T. The dependences are measured for three (001)-grown GaAs/AlGaAs samples with various QW widths under normal incidence of the light at room temperature. Arrows indicate wavelengths used in figure 2.

shift of the spectral position of the photocurrent resonance by variation of the QW width, as well its temperature behaviour demonstrate that the observed photocurrent is caused by the inter-subband transitions.

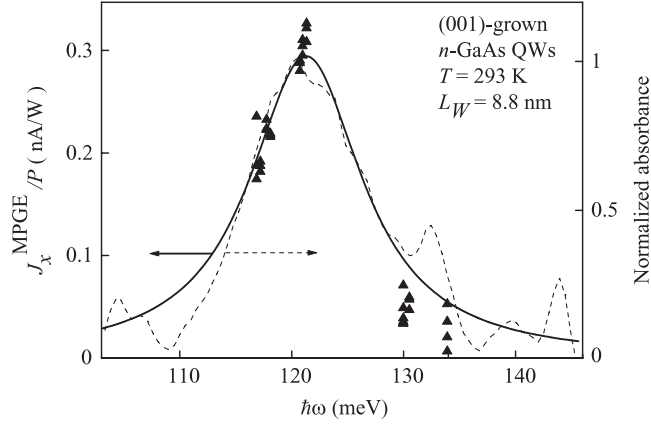


**Figure 5.** Spectral dependence of the magneto-induced photocurrent  $J_x^{\text{MPGE}}$  normalized by the power  $P$  at the magnetic field  $B_y = 0.3$  T. The current is measured under normal incidence of the light at room temperature. The solid curve is the fit to experimental data (triangles) by a Lorentz function. The dashed curve shows the normalized absorbance spectrum measured in the multiple pass geometry.

Now we analyse the dependence of the MPGE photocurrent on the angle of incidence  $\theta_0$  and the azimuth angle  $\alpha$  considering that the QW structure represents an absorbing uniaxial medium with the optical axis perpendicular to the structure surface. We assume that in the investigated samples the anisotropy of the refractive index is sufficiently small ( $n_z \approx n_{\parallel} \approx n$ ), but the anisotropy of the absorbance is strong ( $\eta_z \gg \eta_{\parallel}$ ), where the subscripts  $z$  and  $\parallel$  correspond to the radiation polarized along the growth direction  $z$  and parallel to the QW plane, respectively. In the case of linearly polarized radiation, the polarization dependence of the structure absorbance  $\eta(\alpha, \theta)$  following [36] and the Fresnel laws is described by

$$\eta(\alpha, \theta) = t_p^2 \cos^2 \alpha (\eta_{\parallel} \cos^2 \theta + \eta_z \sin^2 \theta) + t_s^2 \eta_{\parallel} \sin^2 \alpha, \quad (2)$$

where  $\theta$  is the refraction angle in the QW structure,  $\sin \theta = \sin \theta_0 / n$ , and  $t_p$  and  $t_s$  are the transmission coefficients through the sample surface for p- and s-polarized components of the light electric field, respectively [37].

We suppose that the polarization dependence of the MPGE current density is determined solely by the polarization dependence of the radiation absorbance and, therefore, has the form

$$j_x^{\text{MPGE}} = \gamma B_y \frac{nc}{4\pi} E_0^2 \eta(\alpha, \theta), \quad (3)$$

where  $\gamma$  is a parameter,  $E_0$  is the electric field amplitude of incident light and  $c$  is the light velocity. While in the experiments the electric current  $J_x^{\text{MPGE}}$  is measured, in the theoretical consideration the current density  $j_x^{\text{MPGE}}$  is used, which is proportional to the current  $J_x^{\text{MPGE}}$ . We fit the measured polarization dependence of the photocurrent by equations (2) and (3) using, besides the ordinate scaling parameter  $\gamma$ , the ratio  $\eta_z/\eta_{\parallel}$  as a fitting parameter. Figure 3 shows that the MPGE data can be fitted well by equation (2) for  $\eta_z/\eta_{\parallel} \approx 50$ , supporting the assumption that the polarization dependence of the photocurrent can be described solely by the polarization dependence of absorption.

As demonstrated above, in our experiments the current is caused by direct inter-subband transitions which are usually supposed to be excited by light with the polarization vector having a non-zero component normal to the QW plane only (for review, see [38]). In our consideration the corresponding absorbance is  $\eta_z$ . The inter-subband absorption of light polarized parallel

to the QW plane  $\eta_{\parallel}$  is generally expected to vanish because these transitions are forbidden by the dipole selection rules. However, these rules are valid in the framework of the simple one-band model only [39, 40] and it has been demonstrated experimentally that they are not rigorous [41]. Our data support this conclusion and show that the absorbance of light with the polarization vector parallel to the QW plane can be as large as 2% of the absorbance of the light polarized along the QW growth direction.

## 2. Phenomenological analysis

The dependence of the photocurrent direction on the light polarization and orientation of the magnetic field with respect to the crystallographic axes may be obtained from symmetry considerations, which do not require knowledge of the microscopic origin of the effect. In particular, the MPGE current in response to linearly polarized radiation and within the linear regime in the magnetic field is given by [2, 3, 23]

$$j_{\alpha} = \sum_{\beta\gamma\delta} \phi_{\alpha\beta\gamma\delta} B_{\beta} \frac{E_{\gamma} E_{\delta}^{*} + E_{\delta} E_{\gamma}^{*}}{2}, \quad (4)$$

where  $\phi$  is a fourth-rank pseudo-tensor symmetric in the last two indices,  $\phi_{\alpha\beta\gamma\delta} = \phi_{\alpha\beta\delta\gamma}$ , and  $E_{\gamma}$  are components of the electric field of the radiation wave in the structure.

We focus on QWs of  $C_{2v}$  symmetry, which corresponds to asymmetrically doped (001)-oriented GaAs QW structures studied in our experiments. In structures of such a symmetry, components of the MPGE current for, e.g.  $\mathbf{B} \parallel y$  are described by

$$j_x = [C_1(e_x^2 + e_y^2) + C_2(e_x^2 - e_y^2) + C_3 e_z^2] B_y I, \quad (5)$$

$$j_y = C_4 e_x e_y B_y I, \quad (6)$$

where  $(e_x, e_y, e_z)$  are components of the unit polarization vector  $e$  inside the medium,  $e$  is assumed to be real for the linearly polarized radiation;  $I$  is the light intensity inside the medium related to the electric field of the incident light  $E_0$  by  $I = (ncE_0^2/4\pi)[(t_s^2 - t_p^2) \sin^2 \alpha + t_p^2]$ ; and  $C_1/C_4$  are linearly independent coefficients that can be non-zero in QWs of  $C_{2v}$  symmetry, and are related to components of the tensor  $\phi_{\alpha\beta\gamma\delta}$  by  $C_1 \propto (\phi_{xyxx} + \phi_{xyyy})/2$ ,  $C_2 \propto (\phi_{xyxx} - \phi_{xyyy})/2$ ,  $C_3 \propto \phi_{xyzx}$ ,  $C_4 \propto 2\phi_{yyxy} = 2\phi_{yyyx}$ .

The fact that at normal incidence ( $e_z = 0$ ,  $e_x^2 + e_y^2 = 1$ ) we observed only a polarization-independent photocurrent in the direction perpendicular to the magnetic field demonstrates that the coefficients  $C_2$  and  $C_4$  in the present experiments are negligibly small compared to  $C_1$ . At oblique incidence, the polarization-dependent current contribution determined by the coefficient  $C_3$  is also detected. We found from experiment that  $C_3 \gg C_1$ . Such a behaviour is similar to the polarization dependence of the QW absorbance  $\eta$  where, in accordance with equation (2), the radiation polarized in the QW plane causes weaker optical transitions than that having a non-zero out-of-plane component of the polarization vector. As has been shown,  $\mathbf{j}$  can be described solely by the polarization dependence of  $\eta$ . In this model the parameters  $C_1$  and  $C_3$  in the phenomenological expression equation (5) are given by  $C_1 = \gamma \eta_{\parallel}$  and  $C_3 = \gamma \eta_z$ .

## 3. Microscopic theory

Microscopically, the magneto-gyrotropic photocurrents in QW structures can be of both spin-dependent as well as spin-independent origin. The proposed spin-dependent mechanisms of photocurrents include asymmetry of direct optical transitions between Rashba–Dresselhaus spin-split branches of the lowest electron subband [27, 28, 42], spin-dependent asymmetry of

the scattering-assisted radiation absorption by free carriers (Drude absorption) [25], and spin-dependent energy relaxation of the electron gas heated by the radiation [25, 26, 43]. The spin-independent mechanisms reported so far comprise magnetic field induced photocurrents caused by a diamagnetic shift of energy bands [29–32, 38] and diamagnetic corrections to electron–phonon interaction [44, 45]. In this section we consider step by step various microscopic mechanisms which can contribute to the photocurrent induced by optical transitions between the quantum subbands  $e1$  and  $e2$  in the presence of an in-plane magnetic field. We assume for simplicity that the photocurrent is excited at oblique incidence of p-polarized radiation. This particular case can be described in a simple single-band model where only the  $e_z$  component of the polarization vector induces inter-subband optical transitions. In the phenomenological theory this contribution to the current corresponds to the last term on the right-hand side of equation (5) proportional to the parameter  $C_3$ .

### 3.1. Diamagnetic mechanisms of the MPGE caused by inter-subband optical transitions in quantum wells

Diamagnetic mechanisms of the MPGE are related to the influence of the in-plane magnetic field on the orbital motion of carriers rather than on the electron spin. Microscopically, these mechanisms originate from the Lorentz force, which pushes electrons to the right or the left interface depending on their direction of velocity and, therefore, changes the electron wavefunction and energy. Since the Lorentz force is proportional to the magnetic field and the electron velocity, the resulting small diamagnetic corrections to the wavefunction and energy are linear in  $\mathbf{k}$  as well as linear in  $\mathbf{B}$ .

Below, again for simplicity, we consider only linear-in- $\mathbf{k}$  corrections caused by structure inversion asymmetry. The corresponding contribution to the effective Hamiltonian induced by the in-plane magnetic field has the form [38]

$$H_{\text{dia}} = \frac{\hbar e}{m^* c} (B_x k_y - B_y k_x) z, \quad (7)$$

where  $e$  is the electron charge,  $m^*$  is the effective electron mass,  $B_x$  and  $B_y$  are components of the magnetic field, and  $z$  is the coordinate operator. The Hamiltonian equation (7) corresponds to the vector potential  $\mathbf{A} = (B_y z, -B_x z, 0)$ ,  $\mathbf{B} = \text{rot } \mathbf{A}$ .

*3.1.1. Current due to  $\mathbf{k}$ -linear diamagnetic shift of subbands.* It is a well-known fact that an in-plane magnetic field applied to an asymmetric two-dimensional (2D) electron gas induces a spin-independent diamagnetic shift of the electron spectrum in  $\mathbf{k}$ -space in each size-quantized subband [38]. The corresponding corrections to the electron energies are determined by the diagonal matrix elements of the Hamiltonian (7) and have the form

$$\delta \varepsilon_\nu = \frac{\hbar e}{m^* c} (B_x k_y - B_y k_x) z_{\nu\nu}, \quad (8)$$

where  $\nu$  is the subband index,  $z_{\nu\nu} = \int \varphi_\nu^2(z) z \, dz$  is the coordinate matrix element, and  $\varphi_\nu$  is the function of size quantization in the subband  $\nu$  in zero magnetic field. This situation is sketched in figure 6(a) for  $e1$  and  $e2$  subbands. We note that, in spite of the fact that in gyrotropic QWs the spin degeneracy is removed even in the absence of an external magnetic field, we neglect both the zero-field spin-splitting and the Zeeman spin-splitting in the description of diamagnetic mechanisms of the current formation. The value of the diamagnetic shift depends on  $z_{\nu\nu}$  and is generally different for  $e1$  and  $e2$  subbands. Due to the relative shift of the two subbands  $\Delta k_x \propto B_y$ , the inter-subband optical transitions induced by the monochromatic radiation of the photon energy  $\hbar\omega_1$  occur only at a fixed wavevector  $k_{x1}$  where the energy

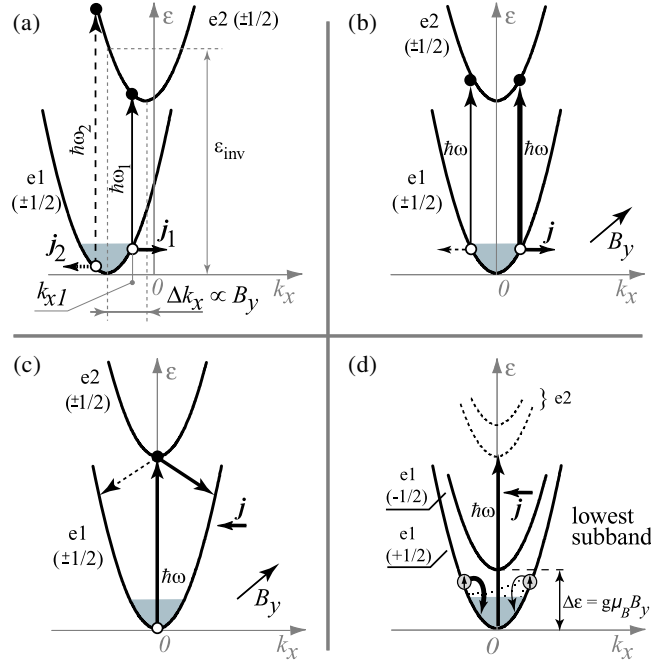


**Figure 6.** Microscopic models of MPGE current formation at inter-subband transitions. ((a) and (b)) Current induced by asymmetric optical excitation due to (a) diamagnetic shift of subbands in  $k$ -space, (b) linear-in- $k$  diamagnetic terms in the optical transition matrix elements. ((c) and (d)) Current induced by asymmetric free carrier relaxation due to (c)  $k$ -linear diamagnetic terms in the scattering amplitude, (d) spin-dependent asymmetry of energy relaxation.

of the incident light matches the transition energy, as is indicated by the solid vertical arrow in figure 6(a). Therefore, optical transitions generate an imbalance in momentum distribution in both subbands, yielding an electric current. However, a non-equilibrium distribution of carriers in the upper subband rapidly relaxes due to the very effective relaxation channel of longitudinal optical (LO) phonon emission, because the energy of the inter-subband optical transition is well above the energy of LO phonons in  $n$ -GaAs QWs ( $\hbar\Omega_{LO} \approx 35$  meV). Thus, the contribution of the  $e2$  subband to the electric current vanishes and the electron flow is determined by the momentum distribution of carriers in the lowest subband. As directly follows from this model picture, the variation in the incident light frequency causes the inversion of the current direction. At small photon energy,  $\hbar\omega_1 < \epsilon_{inv}$ , excitation occurs at  $k_{x1}$  shifted to the right from the  $e1$  minimum, resulting in a current  $j_x$  shown by the solid arrow in figure 6(a). The increase in the photon energy shifts the transition toward negative  $k_x$  ( $\hbar\omega_2 > \epsilon_{inv}$ , dashed vertical arrow in figure 6(a)) and reverses the direction of the current shown by the dashed horizontal arrow. The inversion of the current sign occurs at the photon energy  $\hbar\omega = \epsilon_{inv}$ , corresponding to the optical transitions at the minimum of  $e1$ .

Calculations show that, for the case of optical transitions between the subbands  $e1$  and  $e2$  and the magnetic field aligned along  $y$ , this contribution to the photocurrent has the form

$$j_x = (z_{11} - z_{22}) \frac{e^2 B_y}{m^* c} \left[ \tau_p^{(2)} \eta(\hbar\omega) + (\tau_p^{(1)} - \tau_p^{(2)}) \bar{\epsilon} \frac{d\eta(\hbar\omega)}{d\hbar\omega} \right] \frac{I}{\epsilon_{21}}, \quad (9)$$

where  $\tau_p^{(1)}$  and  $\tau_p^{(2)}$  are the momentum scattering times in the subbands,  $\eta(\hbar\omega)$  is the QW absorbance, which is calculated by neglecting  $k$ -linear terms but taking into account the

inhomogeneous spectral broadening of the inter-subband resonance,  $\varepsilon_{21}$  is the energy separation between the subbands  $e1$  and  $e2$ , and  $\bar{\varepsilon}$  is the average electron kinetic energy. The latter equals  $k_B T$  and  $E_F/2$  for a non-degenerate two-dimensional electron gas and a degenerate two-dimensional electron gas, respectively, where  $T$  is the temperature and  $E_F$  is the Fermi energy.

In accordance with general symmetry arguments, the MPGE current given by equation (9) is related to the structure inversion asymmetry of the QW and vanishes in symmetric structures where  $z_{11} = z_{22}$ . From equation (9) it follows that, for a relaxation time of carriers in the excited subband much shorter than that in the ground subband,  $\tau_p^{(2)} \ll \tau_p^{(1)}$ , the current contribution due to the diamagnetic shift of the electron subbands is proportional to the spectral derivative of the QW absorbance. Hence, spectral investigations of MPGE enable one to evaluate the contribution of this mechanism. We note that the spectral inversion of the current direction is a characteristic feature of some other photocurrents caused by inter-subband transitions in n-doped QW structures which do not require a magnetic field, such as linear [9, 10] and circular [11] photon drag effects as well as the circular photogalvanic [13, 46] effect. In contrast, the contribution to the MPGE photocurrent induced by the inter-band absorption and resulting from the diamagnetic shifts of electron and hole subbands does not share such spectral inversion.

### 3.1.2. Current due to $\mathbf{k}$ -linear diamagnetic terms in the matrix element of optical transitions.

In the previous section we considered the photocurrent caused by linear-in- $\mathbf{k}$  and linear-in- $\mathbf{B}$  terms in the energy spectrum, yielding the diamagnetic shift of subbands. Another diamagnetic contribution to the MPGE, which does not rely on a band shift, comes from the diamagnetic terms in the matrix element of inter-subband optical transitions  $M$ . These terms are also linear in  $\mathbf{k}$  and  $\mathbf{B}$  and result in different probabilities of optical transitions for positive and negative  $k_x$ . Indeed, the in-plane magnetic field intermixes the electron states from the different subbands which leads to asymmetric terms in the matrix element of optical transitions. This is depicted in figure 6(b) by vertical arrows of different thickness. This process leads to an asymmetric distribution of carriers in  $\mathbf{k}$ -space, i.e. to an electrical current. Again, the contribution of the upper subband to the current can be ignored due to rapid relaxation by emission of optical phonons.

In first-order perturbation theory, the wavefunctions of size quantization have the form

$$\varphi_{\nu, \mathbf{k}}(z) = \varphi_{\nu}(z) + (B_x k_y - B_y k_x) \frac{\hbar e}{m^* c} \sum_{\nu' \neq \nu} \frac{z_{\nu' \nu}}{\varepsilon_{\nu \nu'}} \varphi_{\nu'}(z), \quad (10)$$

where  $\varepsilon_{\nu \nu'} = \varepsilon_{\nu} - \varepsilon_{\nu'}$  is the energy separation between the subbands. We note that the functions given by equation (10) with different  $\nu$  remain orthogonal at any wavevector  $\mathbf{k}$  and, therefore, the selection rules for inter-subband optical transitions are preserved. However, the in-plane magnetic field adds  $\mathbf{k}$ -linear terms to the matrix element of optical transitions between the subbands  $e1$  and  $e2$ . This matrix element can be written as

$$M = M_0 \left[ 1 + (B_x k_y - B_y k_x) \frac{\hbar e}{m^* c} \sum_{\nu \neq 1, 2} \left( \frac{z_{\nu 1} p_{\nu 2}}{\varepsilon_{\nu 1} p_{21}} - \frac{z_{\nu 2} p_{\nu 1}}{\varepsilon_{\nu 2} p_{21}} \right) \right], \quad (11)$$

where  $M_0 \propto p_{21} e_z$  is the matrix element of the transitions in zero field, and  $p_{\nu \nu'} = \int \varphi_{\nu}(z) p_z \varphi_{\nu'}(z) dz$  is the matrix element of the momentum operator.

The  $\mathbf{k}$ -linear terms in the matrix element of the optical transitions (11) give rise to an imbalance in the carrier distribution between positive and negative wavevectors in both  $e1$  and  $e2$  subbands, leading to a net electric current. Calculation shows that the corresponding electric

current for the magnetic field  $\mathbf{B}$  aligned along the  $y$  axis is given by

$$j_x = 2(\tau_p^{(1)} - \tau_p^{(2)}) \bar{e} \frac{e^2 B_y}{m^* c} \sum_{v \neq 1,2} \left( \frac{z_{v1} p_{v2}}{\varepsilon_{v1} p_{21}} - \frac{z_{v2} p_{v1}}{\varepsilon_{v2} p_{21}} \right) \frac{I\eta(\hbar\omega)}{\varepsilon_{21}}. \quad (12)$$

The photocurrent given by equation (12) is present only in asymmetric QWs. In symmetric QWs, where the wavefunctions  $\varphi_v(z)$  are either even or odd, the current vanishes because the products  $z_{v1} p_{v2}$  and  $z_{v2} p_{v1}$  are zero for any  $v$ . In contrast to the mechanism considered in section 3.1.1, the spectral behaviour of the photocurrent caused by  $\mathbf{k}$ -linear terms in the optical matrix element follows the QW absorbance. However, estimations show that the contribution described by equation (12) is less than the photocurrent due to the diamagnetic shift of the subbands given by equation (9) and, thus, cannot be responsible for the observed MPGE.

**3.1.3. Current due to  $\mathbf{k}$ -linear diamagnetic terms in the scattering amplitude.** Besides the asymmetry of optical transitions considered above, an asymmetry in the subsequent relaxation processes of photocarriers can also cause an electric current. The relaxation processes following the inter-subband optical excitation include two steps: electron scattering back from the excited  $e2$  to the lower  $e1$  subband and subsequent relaxation to the equilibrium within the  $e1$  subband. The former step, electron scattering to the lower subband, is depicted in figure 6(c) by tilted downward arrows. In gyrotropic quantum wells subjected to an external magnetic field, the matrix element of inter-subband scattering by static defects or phonons contains an additional term proportional to  $(B_x k_y - B_y k_x)$ . Therefore, the scattering rates to final states with positive and negative wavevectors  $k_x$  become different, as reflected in figure 6(c) by arrows of different thickness. Such an imbalance caused by asymmetry of the scattering results in an electric current in the ground subband which is proportional to the applied magnetic field.

To estimate this current contribution we neglect diamagnetic shifts of the subbands and consider electron scattering from the state in the second subband bottom ( $e2, 0$ ) to the state in ground subband ( $e1, \mathbf{k}$ ) assisted by the most efficient process here of an optical phonon emission. Taking into account the form of the electron wavefunctions in the subbands (see equation (10)), one can derive the matrix element of inter-subband scattering. For the Frölich mechanism of electron–phonon interaction [2], it has the form

$$V_{e1,\mathbf{k}; e2,0}^{(+)} = \frac{C}{q} \left[ Q_{12}(q_z) + (B_x k_y - B_y k_x) \frac{\hbar e}{m^* c} \sum_{v \neq 1} \frac{z_{v1}}{\varepsilon_{1v}} Q_{2v}(q_z) \right] \delta_{\mathbf{k}, -\mathbf{q}_{\parallel}}, \quad (13)$$

where  $C$  is a parameter depending on the material,  $Q_{vv'}(q_z) = \int \varphi_v(z) \varphi_{v'}(z) \exp(-iq_z z) dz$ ,  $\mathbf{q} = (\mathbf{q}_{\parallel}, q_z)$  is the wavevector of the phonon involved,  $\mathbf{q}_{\parallel} = -\mathbf{k}$ ,  $k = |\mathbf{k}|$ , and  $k = \sqrt{2m^*(\varepsilon_{21} - \hbar\Omega_{LO})/\hbar}$  due to the energy and the in-plane quasi-momentum conservation.

The matrix element of inter-subband scattering (13) contains  $\mathbf{k}$ -linear terms which lead to an asymmetric distribution of carriers in the ground subband. Calculation shows that the corresponding electric current for the magnetic field  $\mathbf{B}$  aligned along the  $y$  axis has the form

$$j_x = 2\tau_p^{(1)} \frac{e^2 B_y}{m^* c} \left( 1 - \frac{\hbar\Omega}{\varepsilon_{21}} \right) \sum_{v \neq 1} \frac{z_{v1} \zeta_v}{\varepsilon_{v1}} I\eta(\hbar\omega), \quad (14)$$

where

$$\zeta_v = \frac{\int \int \varphi_1(z) \varphi_2(z) \varphi_2(z') \varphi_v(z') \exp(-|z - z'|k) dz dz'}{\int \int \varphi_1(z) \varphi_2(z) \varphi_1(z') \varphi_2(z') \exp(-|z - z'|k) dz dz'}. \quad (15)$$

We note that, in this mechanism, values of  $k$  can be large compared to that in the mechanism of section 3.1.2. Similarly to the previous mechanisms of the MPGE, the current due to the asymmetry of scattering (14) is present only in asymmetric QWs where the products  $z_{v1} \zeta_v$

do not vanish. We also pointed out that processes of energy relaxation of electrons within the ground subband, which follow the inter-subband scattering, are also asymmetrical in the presence of in-plane magnetic field [44, 45] and contribute to the current.

The spectral dependence of relaxation currents repeats that of the QW absorbance  $\eta(\hbar\omega)$ , which is reasonable for all mechanisms where details of optical excitation are lost. Estimations show that these mechanisms can predominate in real structures and determine the MPGE behaviour.

### 3.2. Spin-related mechanisms

This group of the MPGE mechanisms is based on spin-dependent asymmetry of photoexcitation and/or relaxation in the gyrotropic QWs with equilibrium spin polarization due to the Zeeman effect. Two spin-related current contributions considered below follow the spectral dependence of the QW absorbance  $\eta(\hbar\omega)$ .

*3.2.1. Current due to spin-dependent asymmetry of energy relaxation.* This mechanism is considered in detail in [25, 26] for an electron gas heated by the Drude-like absorption of the terahertz radiation. The mechanism is based on the process of energy relaxation and, therefore, does not relate to details of optical excitation, besides the strength of absorption and processes involved in the energy relaxation.

Figure 6(d) sketches the basic physics of this mechanism. In the considered case of radiation absorption due to direct inter-subband transitions, electrons excited to the  $e2$  subband first return to the ground subband and then rapidly lose their energy by the emission of optical phonons. After the emission of optical phonons the energy of the electrons becomes smaller than  $\hbar\Omega_{LO}$  and the relaxation continues due to the emission of acoustic phonons. Due to the Zeeman effect, the lowest subband is split into two spin branches which are unequally occupied. For simplicity, figure 6(d) sketches the process of energy relaxation of hot electrons for only the lowest spin-up branch ( $s = +1/2$ ). Energy relaxation processes are shown by curved arrows. Usually, energy relaxation via scattering of electrons is considered to be spin-independent. In gyrotropic media, however, spin-orbit interaction adds an asymmetric spin-dependent term to the scattering probability. These terms in the scattering matrix element are proportional to components of  $[\boldsymbol{\sigma} \times (\mathbf{k} + \mathbf{k}')]_x$ , where  $\boldsymbol{\sigma}$  is the vector composed of the Pauli matrices, and  $\mathbf{k}$  and  $\mathbf{k}'$  are the initial and scattered electron wavevectors in the ground subband (we consider here only the spin-dependent contribution induced by hetero-potential asymmetry). Due to spin-dependent scattering, transitions to positive and negative  $k'_x$ -states occur with different probabilities. Therefore hot electrons with opposite  $k_x$  within one branch have different relaxation rates. In figure 6(d) this difference is indicated by arrows of different thickness. This in turn yields a net electron flow,  $i_{\pm 1/2}$ , within each spin branch. Since the asymmetric part of the scattering amplitude depends on spin orientation, the probabilities for scattering to positive or negative  $k'_x$ -states are inverted for spin-down and spin-up branches. Without a magnetic field, the charge currents  $j_+ = ei_{+1/2}$  and  $j_- = ei_{-1/2}$  have opposite directions because  $i_{+1/2} = -i_{-1/2}$  and cancel each other. However, the external magnetic field changes the relative population of spin branches and, therefore, lifts the balance between  $j_+$  and  $j_-$ , yielding a net electric current. The photocurrent magnitude can be estimated as

$$j \sim e\tau_p^{(1)} S^{(0)} \frac{\xi}{\hbar} I\eta(\hbar\omega), \quad (16)$$

where  $S^{(0)} = g\mu_B B / (4k_B T)$  is the equilibrium spin polarization for the Boltzmann distribution, and  $\xi$  is a parameter standing for the ratio of spin-dependent to spin-independent parts of electron-phonon interaction.

3.2.2. *Current due to asymmetry of spin relaxation (spin-galvanic effect).* For completeness, we also give an estimation for the second possible spin-dependent mechanism, previously considered by us in [24]. This is based on the asymmetry of spin-flip relaxation processes and represents in fact the spin-galvanic effect [12] where the current is linked to non-equilibrium spin polarization

$$j_i = Q_{ii'}(S_{i'} - S_{i'}^{(0)}). \quad (17)$$

Here  $S$  is the average non-equilibrium electron spin and  $S^{(0)}$  is its equilibrium value; see equation (16). In contrast to the mechanisms considered in sections 3.1.1–3.1.3, this mechanism requires spin-flip processes together with a *non-equilibrium* spin polarization. A *non-equilibrium* spin polarization results from the photoinduced depolarization of electron spins in the system with equilibrium polarization caused by the Zeeman effect. Indeed, due to the fact that, in equilibrium, electrons preferably occupy the lower spin branch, optical transitions, being proportional to the electron concentration, predominantly excite this branch. These optically excited electrons under energy relaxation return to both spin branches, resulting in non-equilibrium population of the branches. The following spin relaxation results in the spin-galvanic current (see [12]).

An estimation of this photocurrent for the D'yakonov–Perel spin relaxation mechanism yields

$$j \sim e\tau_p^{(1)} S^{(0)} \frac{\beta^{(1)}}{\hbar} \frac{I\eta(\hbar\omega)}{\varepsilon_{21}}, \quad (18)$$

where  $\beta$  is the constant of  $k$ -linear spin–orbit splitting of the subband  $e1$ .

#### 4. Conclusions

Summarizing our experiments and the microscopic theory developed here, we emphasize that the resonant spectral behaviour of the observed magnetic field induced photocurrent following the inter-subband absorption profile proves that the photocurrent is due to direct inter-subband transitions. As an interesting feature, the resonant photocurrent is also detected at normal incidence of the radiation on (001)-grown QWs. This result demonstrates that the selection rules conventionally applied for inter-subband optical transitions are not rigorous. Considering that the photocurrent is proportional to the QW absorbance, we obtain from the experiment that the ratio of absorbance for light polarized along the growth direction  $z$  and in the QW plane is  $\eta_z/\eta_{\parallel} \approx 50$ . Surprisingly, the MPGE photocurrent is not caused by the diamagnetic shift of subbands (see section 3.1.1). Such a current has been reported previously for inter-band absorption and is expected to be strong compared to a spin-dependent mechanism because of its non-relativistic nature. However, the absence of spectral inversion of the photocurrent at inter-subband absorption resonance unambiguously rules out this mechanism. Three other possible mechanisms of current formation developed here cannot be distinguished qualitatively. Based on quantitative estimations of the mechanisms given in sections from 3.1.2 to 3.2.2, we attribute the MPGE current to  $k$ -linear diamagnetic terms in the scattering matrix element, yielding asymmetric relaxation of carriers in  $k$ -space (section 3.1.3). Finally, we note that diamagnetic and spin-dependent mechanisms might be qualitatively distinguished in structures where the  $g$ -factor can be varied, like in dilute semimagnetic materials. Indeed, while spin-dependent mechanisms are proportional to the  $g$ -factor, diamagnetic mechanisms are independent of the Zeeman splitting.

#### Acknowledgments

We thank E L Ivchenko for helpful discussions. This work was supported by the Deutsche Forschungsgemeinschaft through GA 501/6, SFB 689, SPP 1285, the Russian Foundation

for Basic Research, programs of the Russian Academy of Science and Russian Ministry of Education and Science, the Russian President Grant for young scientists, and the Russian Science Support Foundation.

## References

- [1] Ganichev S D and Prettl W 2003 *J. Phys.: Condens. Matter* **15** R935
- [2] Ivchenko E L 2005 *Optical Spectroscopy of Semiconductor Nanostructures* (Harrow: Alpha Science Int.)
- [3] Ganichev S D and Prettl W 2006 *Intense Terahertz Excitation of Semiconductors* (Oxford: Oxford University Press)
- [4] Gusev G M, Kvon Z D, Magarill L I, Palkin A M, Sozinov V I, Shegai O A and Entin M V 1987 *Pis. Zh. Eksp. Teor. Fiz.* **46** 28  
Gusev G M, Kvon Z D, Magarill L I, Palkin A M, Sozinov V I, Shegai O A and Entin M V 1987 *Sov. Phys.—JETP Lett.* **46** 33 (Engl. Transl.)
- [5] Ganichev S D, Ivchenko E L, Danilov S N, Eroms J, Wegscheider W, Weiss D and Prettl W 2001 *Phys. Rev. Lett.* **86** 4358
- [6] Bieler M, Laman N, van Driel H M and Smirl A L 2005 *Appl. Phys. Lett.* **86** 061102
- [7] Yang C L, He H T, Ding L, Cui L J, Zeng Y P, Wang J N and Ge W K 2006 *Phys. Rev. Lett.* **96** 186605
- [8] Cho K S, Chen Y F, Tang Y Q and Shen B 2007 *Appl. Phys. Lett.* **90** 41909
- [9] Luryi S 1987 *Phys. Rev. Lett.* **58** 2263
- [10] Wieck A D, Sigg H and Ploog K 1990 *Phys. Rev. Lett.* **64** 463
- [11] Shalygin V A *et al* 2006 *JETP Lett.* **84** 570
- [12] Ganichev S D, Ivchenko E L, Bel'kov V V, Tarasenko S A, Sollinger M, Weiss D, Wegscheider W and Prettl W 2002 *Nature* **417** 153
- [13] Ganichev S D *et al* 2003 *Phys. Rev. B* **68** R081302
- [14] Bhat R D R and Sipe J E 2000 *Phys. Rev. Lett.* **85** 5432
- [15] Stevens M J, Smirl A L, Bhat R D R, Sipe J E and van Driel H M 2002 *J. Appl. Phys.* **91** 4382
- [16] Hübner J, Rühle W W, Klude M, Hommel D, Bhat R D R, Sipe J E and van Driel H M 2003 *Phys. Rev. Lett.* **90** 216601
- [17] Stevens M J, Smirl A L, Bhat R D R, Najimaie A, Sipe J E and van Driel H M 2003 *Phys. Rev. Lett.* **90** 136603
- [18] Entin M V 1989 *Fiz. Tekh. Poluprovodn.* **23** 1066  
Entin M V 1989 *Sov. Phys.—Semicond.* **23** 664 (Engl. Transl.)
- [19] Magarill L I 2001 *Physica E* **9** 652
- [20] Ganichev S D *et al* 2004 *Phys. Rev. Lett.* **92** 256601
- [21] Giglberger S *et al* 2007 *Phys. Rev. B* **75** 035327
- [22] Andrianov A V and Yaroshetskii I D 1984 *Pis. Zh. Eksp. Teor. Fiz.* **40** 131  
Andrianov A V and Yaroshetskii I D 1984 *Sov. Phys.—JETP Lett.* **40** 882 (Engl. Transl.)
- [23] Sturm B I and Fridkin V M 1992 *The Photovoltaic and Photorefractive Effects in Non-Centrosymmetric Materials* (New York: Gordon and Breach)
- [24] Bel'kov V V *et al* 2005 *J. Phys.: Condens. Matter* **17** 3405
- [25] Ganichev S D *et al* 2006 *Nat. Phys.* **2** 609
- [26] Ganichev S D *et al* 2007 *Phys. Rev. B* **75** 155317
- [27] Magarill L I 1990 *Fiz. Tverd. Tela* **32** 3558  
Magarill L I 1990 *Sov. Phys.—Solid State* **32** 2064 (Engl. Transl.)
- [28] Dmitriev A P, Emel'yanov S A, Ivanov S V, Kop'ev P S, Terent'ev Ya V and Yaroshetskii I D 1991 *Pis. Zh. Eksp. Teor. Fiz.* **54** 279  
Dmitriev A P, Emel'yanov S A, Ivanov S V, Kop'ev P S, Terent'ev Ya V and Yaroshetskii I D 1991 *JETP Lett.* **54** 273 (Engl. Transl.)
- [29] Gorbatshevich A A, Kapaev V V and Kopaev Yu V 1993 *Pis. Zh. Eksp. Teor. Fiz.* **57** 565  
Gorbatshevich A A, Kapaev V V and Kopaev Yu V 1993 *JETP Lett.* **57** 580 (Engl. Transl.)
- [30] Aleshchenko Yu A, Voronova I D, Grishechkina S P, Kapaev V V, Kopaev Yu V, Kucherenko I V, Kadushkin V I and Fomichev S I 1993 *Pis. Zh. Eksp. Teor. Fiz.* **58** 377  
Aleshchenko Yu A, Voronova I D, Grishechkina S P, Kapaev V V, Kopaev Yu V, Kucherenko I V, Kadushkin V I and Fomichev S I 1993 *JETP Lett.* **58** 384 (Engl. Transl.)
- [31] Kucherenko I V, Vodop'yanov L K and Kadushkin V I 1997 *Fiz. Tekh. Poluprovodn.* **31** 872  
Kucherenko I V, Vodop'yanov L K and Kadushkin V I 1997 *Semiconductors* **31** 740 (Engl. Transl.)
- [32] Kibis O V 1997 *Pis. Zh. Eksp. Teor. Fiz.* **66** 551  
Kibis O V 1997 *JETP Lett.* **66** 588 (Engl. Transl.)

- [33] Hilber W, Helm M, Alavi K and Pathak R N 1997 *Superlatt. Microstruct.* **21** 85
- [34] Tsujino S, Rüfenacht M, Nakajima H, Noda T, Metzner C and Sakaki H 2000 *Phys. Rev. B* **62** 1560
- [35] Svelto O 1998 *Principles of Lasers* (New York: Plenum)
- [36] Born M and Wolf E 1999 *Principles of Optics* (Cambridge: Cambridge University Press) pp 840–3
- [37] Guenther R D 1990 *Modern Optics* (New York: Wiley) pp 70–1
- [38] Ando T, Fowler A B and Stern F 1982 *Rev. Mod. Phys.* **54** 437
- [39] Warburton R J, Gauer C, Wixforth A, Kotthaus J P, Brar B and Kroemer H 1996 *Phys. Rev. B* **53** 7903
- [40] Ivchenko E L and Tarasenko S A 2004 *Zh. Eksp. Teor. Fiz.* **126** 426  
Ivchenko E L and Tarasenko S A 2004 *JETP* **99** 379 (Engl. Transl.)
- [41] Liu H C, Buchanan M and Wasilewski Z R 1998 *Appl. Phys. Lett.* **72** 1682
- [42] Emel'yanov S A, Terent'ev Ya V, Dmitriev A P and Mel'tser B Ya 1998 *Pis. Zh. Eksp. Teor. Fiz.* **68** 768  
Emel'yanov S A, Terent'ev Ya V, Dmitriev A P and Mel'tser B Ya 1998 *JETP Lett.* **68** 810 (Engl. Transl.)
- [43] Ivchenko E L and Pikus G E 1983 *Izv. Akad. Nauk SSSR Ser. Fiz.* **47** 2369  
Ivchenko E L and Pikus G E 1983 *Bull. Acad. Sci. USSR Phys. Ser.* **47** 81 (Engl. Transl.)
- [44] Kibis O V 1998 *Phys. Lett. A* **244** 432
- [45] Pogosov A G, Budantsev M V, Kibis O V, Pouydebasque A, Maude D K and Portal J C 2000 *Phys. Rev. B* **61** 15603
- [46] Ganichev S D, Bel'kov V V, Schneider P, Ivchenko E L, Tarasenko S A, Schuh D, Wegscheider W, Weiss D and Prettl W 2003 *Phys. Rev. B* **68** 035319